Geomechanics and Engineering, *Vol. 26, No. 6 (2021) 607-615*
https://doi.org/10.12989/gae.2021.26.6.607

Study on the characteristics of wave propagation in functionally graded porous square plates

Hang Xiao[1], Kunming Yan[2] and Guilin She*[3]

[1]*College of Mechanical and Electrical Engineering, Changsha University, Changsha 410022, China*
[2]*China Aviation Changsha Design and Research Co. Ltd, Changsha, 410018, China*
[3]*College of Mechanical and Vehicle Engineering, Chongqing University, Chongqing 400044, China*

(Received June 16, 2021, Revised September 4, 2021, Accepted September 27, 2021)

Abstract. Considering the modified power function form of material parameters, the wave equation of porous functionally graded material plate was established according to Hamilton principle based on the concept of physical medium surface and Reddy high-order shear deformed plate theory. The dispersion relations of five different elastic waves were obtained by using eigenvalue method. Then, the effects of functional gradient index and porosity on the propagation characteristics of five kinds of elastic waves are discussed. Finally, it is found that the pore volume fraction can simultaneously characterize the stiffness strengthening effect and stiffness softening effect, which depends on the power law index.

Keywords: functionally graded material; physical neutral surface concept; wave propagation; porosity

1. Introduction

The wave propagation analysis of structures has attracted the interest of many researchers. This is because the wave problem can effectively detect structural damage. For structures, there are often various forms of waves, for example, for Euler beams, there are only longitudinal and bending waves. For Timoshenko beams, there are three different types of waves, including longitudinal waves, shear waves and bending waves. Similarly, for high-order shear deformed beams, like Timoshenko beams, there are three kinds of elastic waves, including longitudinal wave, shear wave and bending wave. Similarly, for a classical plate, similar to an Euler beam, there are only longitudinal waves (U and V) and curved waves (W). Obviously, the difference between a plate and a beam is that the longitudinal waves in a plate contain two kinds, U and V, where U and V represent the longitudinal waves propagating along the X and Y directions respectively. It can be seen that the characteristics of wave propagation in the classical plate are different from those in the classical beam. That is to say, there are three kinds of waves in the classical plate, including two longitudinal waves and a curved wave. For the first order shear deformed plate, there are five different types of waves, of which two are longitudinal waves, the other two are shear waves, and the last one is bending waves. For Reddy's high-order shear deformed plate theory, it is obvious that, just like the first-order shear deformed plate theory, there are two longitudinal waves, two shear waves and one bending wave. Because the high-order shear deformed plate contains five independent displacement variables, the research literature on wave propagation is less than that of the beam structure and the classical deformed plate. Therefore, it is necessary to study the five waves with different properties in the high-order shear deformed plate.

For instances, Liang and Wang (2020) studied the bending wave of porous FG sandwich plates via a new plate theory, however, they only studied the bending wave, the propagation characteristics of compressional and shear waves were ignored by them. Ebrahimi and Seyfi (2020) studied the bending wave of porous FG plates in thermal environment via the analytical method, however, like Liang and Wang (2020), they only studied the bending wave, the propagation characteristics of compressional and shear waves were ignored by them. Bennai *et al.* (2019) used a four variable plate theory to investigate the bending wave of FG plates with porosities, also, they ignore the longitudinal and shear waves in their paper. Yahia *et al.* (2015) used various plate theories to analyze the bending wave of the porous FG plates. Nebab *et al.* (2019) used higher order shear deformation plate theory to discuss the bending wave of FG plates laid on elastic foundations. Gao *et al.* (2020) studied the bending wave propagation in functionally graded porous plates reinforced with graphene platelets, obviously, again, they didn't study P-waves and shear waves.

During the manufacturing process of functionally graded (FG) materials, pores will be produced. Many scholars have studied the effect of porosities on the functional graded structures. Alnujaie *et al.* (2021) studied the effect of porosity on the forced vibration of FG beams. Khazaei and Mohammadimehr (2020) used the nonlocal strain gradient theory to study the bending and buckling of porous plates considering piezoelectric effects. Mirjavadi *et al.* (2020) used the Airy stress function method to analyze the porosity on the post-buckling behavior of the doubly

*Corresponding author, Professor
E-mail: sheguilin@cqu.edu.cn

ISSN: 2005-307X (Print), 2092-6219 (Online)

curved shells. Sadoughifar *et al.* (2020) adopted the modified couple stresses theory to discuss the buckling behavior of porous annular plates resting on elastic foundations. Mekerbi *et al.* (2019) discussed the thermal buckling of porous FG plates laid on the resting on elastic foundations. Rabia *et al.* (2019) investigated the effect of porosity on FGM beams reinforced with porous functionally graded materials. More works can be found in these relevant papers, for examples, Hadj *et al.* (2019), Ebrahim *et al.* (2019), Arefi and Meskini (2019), Hamed *et al.* (2019), Arshid *et al.* (2019), Benahmed *et al.* (2019), Hadji *et al.* (2019), Fenjan *et al.* (2020), Bamdad *et al.* (2020), Ghandourh and Abdraboh (2020), Jia *et al.* (2020), Batou *et al.* (2019),Civalek *et al.* (2020), Sadoughifar *et al.* (2019), Xu *et al.* (2019), Rahmani *et al.* (2019), Ahmadi and Foroutan (2019), Avcar *et al.* (2019), Jalaei and Civalek (2019), Barretta and de Sciarra, (2019), Faghidian *et al.*(2020), 2021, Ahmed *et al.* (2019), Ghayesh and Farokhi (2020), Farokhi and Ghayesh (2021), Arefi and Zenkour(2017), Arefi *et al.* (2020), Arefi *et al.* (2019), Arefi *et al.* (2016), Lu *et al.* (2019), Lu *et al.* (2021a), Lu *et al.* (2021b),Malikan *et al.* (2020a), Malikan *et al.* (2020b), Zhang *et al.* (2021).

Through literature search, we found that there are some literatures on the characteristics of wave propagation in porous FG plates, but these literatures all have this defect, that is, they only study the bending wave, and lack the research on other types of wave propagation. In order to solve this problem, this paper studies the propagation characteristics of five different types of waves in the porous FG plates for the first time. To this end, we were based on higher order beam theory and used eigenvalue method to analyze five kinds of waves in the porous FG plates.

2. Mechanical model

Consider a functionally graded plate, the top and bottom materials are ceramic and metal respectively, and the thickness of the plate is h, as shown in Fig. 1. We assume the elastic modulus *E*, Poisson ratio v,and the mass density ρ have the form as(Liang and Wang 2020, Ebrahimi and Seyfi 2020, Bennai *et al.* 2019, Yahia *et al.* 2015, Nebab *et al.* 2019)

$$\begin{aligned} E(z) &= [E_t - E_b](\frac{2z+h}{2h})^N + E_b - \frac{\beta}{2}[E_t + E_b] \\ \nu &= [\nu_t - \nu_b](\frac{2z+h}{2h})^N + \nu_b - \frac{\beta}{2}[\nu_t + \nu_b] \\ \rho &= [\rho_t - \rho_b](\frac{2z+h}{2h})^N + \rho_b - \frac{\beta}{2}[\rho_t + \rho_b] \end{aligned} \tag{1a}$$

And in this paper,

$$\begin{aligned} &E_t = 207.79\text{GPa},\ E_b = 322.27\text{GPa}; \\ &\rho_t = 8166\text{Kg/m}^3,\ \rho_b = 2307\text{Kg/m}^3; \\ &\nu_t = \nu_b = 0.3 \end{aligned} \tag{1b}$$

In addition, because the neutral axis and centroid axis of functionally graded materials are not in the same position, the tension-bending coupling effect of functionally graded beams or functionally graded plates will occur. But the physical neutral surface bring structural mechanics analysis

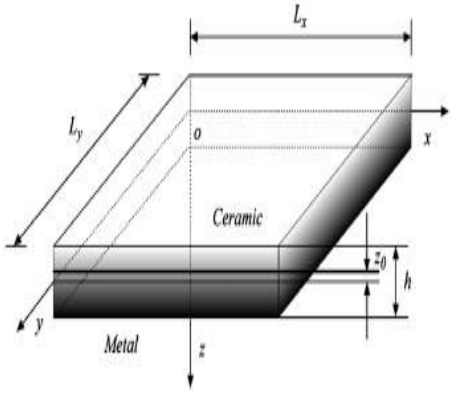

Fig. 1 Coordinate system of functionally graded plate based on physical neutral surface concept (Zhang *et al.* 2013)

of a lot of convenience, because of the stretch bending coupling effect, so based on the analysis of structural vibration, buckling and wave propagation problems, makes the derivation of the equations become very complicated, but once the concept introduced in the physical plane, all the problem solved, at this point, will make the stretch bending coupling effect will disappear, This will make the functionally graded beam or functionally graded plate exhibit the same mathematical and mechanical characteristics as the single material. In many literatures, the concept of physical middle plane is used to study the mechanical properties of functionally graded beam and plate structures.

Based on the concept of physical neutral surface and the theory of Reddy' high-order shear deformation plate, the displacement components are assumed to be (Zhang 2013, 2014)

$$\begin{aligned} u(x,y,z,t) &= u_0(x,y,t) + (z-z_0)\varphi_x(x,y,t) \\ &\quad -\frac{4}{3h^2}(z-c_0)^3(\varphi_x + \frac{\partial w_0}{\partial x}) \\ v(x,y,z,t) &= v_0(x,y,t) + (z-z_0)\varphi_y(x,y,t) \\ &\quad -\frac{4}{3h^2}(z-c_0)^3(\varphi_y + \frac{\partial w_0}{\partial y}) \\ w(x,y,z,t) &= w_0(x,y,t) \end{aligned} \tag{2a}$$

Here, u_0, v_0 and w_0 are the displacement along the *x*, *y* and z directions, φ_x and φy are the rotation along the*x*and *y* direction, *t* stands for the time, and (Zhang 2013, 2014)

$$[z_0, c_0] = \frac{\int_{-h/2}^{h/2}[z, z^3]E(z)dz}{\int_{-h/2}^{h/2}E(z)dz} \tag{2b}$$

The linear strain component is

$$\begin{Bmatrix} \varepsilon_x \\ \varepsilon_y \\ \varepsilon_{xy} \end{Bmatrix} = \begin{Bmatrix} \frac{\partial u_0}{\partial x} \\ \frac{\partial v_0}{\partial y} \\ \frac{\partial u_0}{\partial y} + \frac{\partial v_0}{\partial x} \end{Bmatrix} + (z-z_0)\begin{Bmatrix} \frac{\partial \varphi_x}{\partial x} \\ \frac{\partial \varphi_y}{\partial y} \\ \frac{\partial \varphi_x}{\partial y} + \frac{\partial \varphi_y}{\partial x} \end{Bmatrix} \tag{3}$$

$$-\frac{4}{3h^2}\left(z-c_0\right)^3\begin{Bmatrix}\dfrac{\partial\varphi_x}{\partial x}+\dfrac{\partial^2 w_0}{\partial x^2}\\ \dfrac{\partial\varphi_y}{\partial y}+\dfrac{\partial^2 w_0}{\partial y^2}\\ \dfrac{\partial\varphi_x}{\partial y}+\dfrac{\partial\varphi_y}{\partial x}+2\dfrac{\partial^2 w_0}{\partial x\partial y}\end{Bmatrix},$$
$$\begin{Bmatrix}\varepsilon_{xz}\\ \varepsilon_{yz}\end{Bmatrix}=\begin{Bmatrix}\varphi_x+\dfrac{\partial w_0}{\partial x}\\ \varphi_y+\dfrac{\partial w_0}{\partial y}\end{Bmatrix}-\frac{4}{h^2}\left(z-c_0\right)^2\begin{Bmatrix}\varphi_x+\dfrac{\partial w_0}{\partial x}\\ \varphi_y+\dfrac{\partial w_0}{\partial y}\end{Bmatrix} \tag{3}$$

The stress-strain relationship can be expressed in the form of matrix, as

$$\begin{Bmatrix}\sigma_x\\ \sigma_y\\ \sigma_{xy}\\ \sigma_{xz}\\ \sigma_{yz}\end{Bmatrix}=\begin{bmatrix}\dfrac{E(z)}{1-\nu^2} & \dfrac{\nu(z)E(z)}{1-\nu^2} & 0 & 0 & 0\\ \dfrac{\nu(z)E(z)}{1-\nu^2} & \dfrac{E(z)}{1-\nu^2} & 0 & 0 & 0\\ 0 & 0 & \dfrac{E(z)}{2(1+\nu)} & 0 & 0\\ 0 & 0 & 0 & \dfrac{E(z)}{2(1+\nu)} & 0\\ 0 & 0 & 0 & 0 & \dfrac{E(z)}{2(1+\nu)}\end{bmatrix}\left\{\begin{Bmatrix}\varepsilon_x\\ \varepsilon_y\\ \varepsilon_{xy}\\ \varepsilon_{xz}\\ \varepsilon_{yz}\end{Bmatrix}\right\} \tag{4}$$

Considering the physical mid-plane concept, the coupling effects of tension and bending disappears, and Using Hamilton principle, the wave equation can be deduced as,

$$A_{11}\frac{\partial^2 u_0}{\partial x^2}+A_{12}\frac{\partial^2 v_0}{\partial x\partial y}+A_{66}\left(\frac{\partial^2 u_0}{\partial y^2}+\frac{\partial^2 v_0}{\partial x\partial y}\right)=I_0\frac{\partial^2 u_0}{\partial t^2}$$
$$+J_1\frac{\partial^2\varphi_x}{\partial t^2}-\frac{4I_3}{3h^2}\frac{\partial^2}{\partial t^2}\left(\frac{\partial w_0}{\partial x}\right), \tag{5}$$

$$A_{12}\frac{\partial^2 u_0}{\partial x\partial y}+A_{22}\frac{\partial^2 v_0}{\partial y^2}+A_{66}\left(\frac{\partial^2 u_0}{\partial x\partial y}+\frac{\partial^2 v_0}{\partial x^2}\right)=I_0\frac{\partial^2 v_0}{\partial t^2}$$
$$+J_1\frac{\partial^2\varphi_y}{\partial t^2}-\frac{4I_3}{3h^2}\frac{\partial^2}{\partial t^2}\left(\frac{\partial w_0}{\partial y}\right), \tag{6}$$

$$\left(A_{44}-\frac{8}{h^2}D_{44}+\frac{16}{h^4}F_{44}\right)\left(\frac{\partial\varphi_x}{\partial x}+\frac{\partial^2 w_0}{\partial x^2}\right)+\left(A_{55}\right.$$
$$\left.-\frac{8}{h^2}D_{55}+\frac{16}{h^4}F_{55}\right)\left(\frac{\partial\varphi_y}{\partial y}+\frac{\partial^2 w_0}{\partial y^2}\right)+\frac{4}{3h^2}F_{11}\frac{\partial^3\varphi_x}{\partial x^3}$$
$$+\frac{4}{3h^2}F_{12}\frac{\partial^3\varphi_y}{\partial x^2\partial y}-\frac{16}{9h^4}H_{11}\left(\frac{\partial^3\varphi_x}{\partial x^3}+\frac{\partial^4 w_0}{\partial x^4}\right)$$
$$-\frac{16}{9h^4}H_{12}\left(\frac{\partial^3\varphi_y}{\partial x^2\partial y}+\frac{\partial^4 w_0}{\partial x^2\partial y^2}\right)+\frac{8}{3h^2}F_{66}\left(\frac{\partial^3\varphi_x}{\partial x\partial y^2}\right.$$
$$\left.+\frac{\partial^3\varphi_y}{\partial x^2\partial y}\right)-\frac{32}{9h^4}H_{66}\left(\frac{\partial^3\varphi_x}{\partial x\partial y^2}+\frac{\partial^3\varphi_y}{\partial x^2\partial y}+2\frac{\partial^4 w_0}{\partial x^2\partial y^2}\right)$$
$$+\frac{4}{3h^2}F_{12}\frac{\partial^3\varphi_x}{\partial x\partial y^2}+\frac{4}{3h^2}F_{22}\frac{\partial^3\varphi_y}{\partial y^3}$$
$$-\frac{16}{9h^4}H_{12}\left(\frac{\partial^3\varphi_x}{\partial x\partial y^2}+\frac{\partial^4 w_0}{\partial x^2\partial y^2}\right)-\frac{16}{9h^4}H_{22}\left(\frac{\partial^3\varphi_y}{\partial y^3}\right.$$
$$\left.+\frac{\partial^4 w_0}{\partial y^4}\right)=I_0\frac{\partial^2 w_0}{\partial t^2}-\frac{16}{9h^4}I_6\frac{\partial^2}{\partial t^2}\left(\frac{\partial^2 w_0}{\partial x^2}+\frac{\partial^2 w_0}{\partial y^2}\right)$$
$$+\frac{4}{3h^2}\left[I_3\frac{\partial^2}{\partial t^2}\left(\frac{\partial u_0}{\partial x}+\frac{\partial v_0}{\partial y}\right)+J_4\frac{\partial^2}{\partial t^2}\left(\frac{\partial\varphi_x}{\partial x}+\frac{\partial\varphi_y}{\partial y}\right)\right] \tag{7}$$

$$D_{11}\frac{\partial^2\varphi_x}{\partial x^2}+D_{12}\frac{\partial^2\varphi_y}{\partial x\partial y}-\frac{4}{3h^2}F_{11}\left(\frac{\partial^2\varphi_x}{\partial x^2}+\frac{\partial^3 w_0}{\partial x^3}\right)$$
$$-\frac{4}{3h^2}F_{12}\left(\frac{\partial^2\varphi_y}{\partial x\partial y}+\frac{\partial^3 w_0}{\partial x\partial y^2}\right)+D_{66}\left(\frac{\partial^2\varphi_x}{\partial y^2}+\frac{\partial^2\varphi_y}{\partial x\partial y}\right)$$
$$-\frac{4}{3h^2}F_{66}\left(\frac{\partial^2\varphi_x}{\partial y^2}+\frac{\partial^2\varphi_y}{\partial x\partial y}+2\frac{\partial^3 w_0}{\partial x\partial y^2}\right)$$
$$-\frac{4}{3h^2}F_{11}\frac{\partial^2\varphi_x}{\partial x^2}-\left(A_{44}+\frac{8}{h^2}D_{44}-\frac{16}{h^4}F_{44}\right)$$
$$\times\left(\varphi_x+\frac{\partial w_0}{\partial x}\right)-\frac{4}{3h^2}F_{12}\frac{\partial^2\varphi_y}{\partial x\partial y}$$
$$+\frac{16}{9h^4}H_{11}\left(\frac{\partial^2\varphi_x}{\partial x^2}+\frac{\partial^3 w_0}{\partial x^3}\right)+\frac{16}{9h^4}H_{12}\left(\frac{\partial^2\varphi_y}{\partial x\partial y}\right.$$
$$\left.+\frac{\partial^3 w_0}{\partial x\partial y^2}\right)-\frac{4}{3h^2}F_{66}\left(\frac{\partial^2\varphi_x}{\partial y^2}+\frac{\partial^2\varphi_y}{\partial x\partial y}\right)$$
$$+\frac{16}{9h^4}H_{66}\left(\frac{\partial^2\varphi_x}{\partial y^2}+\frac{\partial^2\varphi_y}{\partial x\partial y}+2\frac{\partial^3 w_0}{\partial x\partial y^2}\right)$$
$$=\frac{\partial^2}{\partial t^2}\left(J_1u_0+K_2\varphi_x-\frac{4}{3h^2}J_4\frac{\partial w_0}{\partial x}\right) \tag{8}$$

$$D_{12}\frac{\partial^2\varphi_x}{\partial x\partial y}+D_{22}\frac{\partial^2\varphi_y}{\partial y^2}-\frac{4}{3h^2}F_{12}\left(\frac{\partial^2\varphi_x}{\partial x\partial y}+\frac{\partial^3 w_0}{\partial x^2\partial y}\right)$$
$$-\frac{4}{3h^2}F_{22}\left(\frac{\partial^2\varphi_y}{\partial y^2}+\frac{\partial^3 w_0}{\partial y^3}\right)+D_{66}\left(\frac{\partial^2\varphi_x}{\partial x\partial y}+\frac{\partial^2\varphi_y}{\partial x^2}\right)$$
$$-\frac{4}{3h^2}F_{66}\left(\frac{\partial^2\varphi_x}{\partial x\partial y}+\frac{\partial^2\varphi_y}{\partial x^2}+2\frac{\partial^3 w_0}{\partial x^2\partial y}\right)$$
$$-\frac{4}{3h^2}F_{22}\frac{\partial^2\varphi_y}{\partial y^2}-\left(A_{55}-\frac{8}{h^2}D_{55}+\frac{16}{h^4}F_{55}\right)$$
$$\times\left(\varphi_y+\frac{\partial w_0}{\partial y}\right)-\frac{4}{3h^2}F_{12}\frac{\partial^2\varphi_x}{\partial x\partial y}+\frac{16}{9h^4}H_{12}\left(\frac{\partial^2\varphi_x}{\partial x\partial y}\right.$$
$$\left.+\frac{\partial^3 w_0}{\partial x^2\partial y}\right)+\frac{16}{9h^4}H_{22}\left(\frac{\partial^2\varphi_y}{\partial y^2}+\frac{\partial^3 w_0}{\partial y^3}\right)$$
$$-\frac{4}{3h^2}F_{66}\left(\frac{\partial^2\varphi_x}{\partial x\partial y}+\frac{\partial^2\varphi_y}{\partial x^2}\right)+\frac{16}{9h^4}H_{66}\left(\frac{\partial^2\varphi_x}{\partial x\partial y}\right.$$
$$\left.+\frac{\partial^2\varphi_y}{\partial x^2}+2\frac{\partial^3 w_0}{\partial x^2\partial y}\right)=\frac{\partial^2}{\partial t^2}\left(J_1v_0+K_2\varphi_y-\frac{4}{3h^2}J_4\frac{\partial w_0}{\partial y}\right) \tag{9}$$

Herein

$$\begin{bmatrix}A_{44}\\ D_{44}\\ F_{44}\end{bmatrix}=\begin{bmatrix}A_{55}\\ D_{55}\\ F_{55}\end{bmatrix}=\begin{bmatrix}A_{66}\\ D_{66}\\ F_{66}\end{bmatrix}=\int_{-\frac{h}{2}}^{\frac{h}{2}}\frac{E(z)}{2(1+\nu)}\begin{bmatrix}1\\ \left(z-z_0\right)^2\\ \left(z-z_0\right)^4\end{bmatrix}\mathrm{d}z$$
$$\begin{bmatrix}A_{11}\\ D_{11}\\ F_{11}\\ H_{11}\end{bmatrix}=\begin{bmatrix}A_{22}\\ D_{22}\\ F_{22}\\ H_{22}\end{bmatrix}=\int_{-\frac{h}{2}}^{\frac{h}{2}}\frac{E(z)}{1-\nu^2}\begin{bmatrix}1\\ \left(z-z_0\right)^2\\ \left(z-z_0\right)^4\\ \left(z-z_0\right)^6\end{bmatrix}\mathrm{d}z \tag{10}$$

$$\begin{bmatrix} A_{12} \\ D_{12} \\ F_{12} \\ H_{12} \end{bmatrix} = \int_{-\frac{h}{2}}^{\frac{h}{2}} \frac{\nu(z)E(z)}{1-\nu^2} \begin{bmatrix} 1 \\ (z-z_0)^2 \\ (z-z_0)^4 \\ (z-z_0)^6 \end{bmatrix} \mathrm{d}z$$

$$\begin{bmatrix} I_0 \\ I_1 \\ I_2 \\ I_3 \\ I_4 \\ I_6 \end{bmatrix} = \int_{-\frac{h}{2}}^{\frac{h}{2}} \rho(z) \begin{bmatrix} 1 \\ (z-z_0) \\ (z-z_0)^2 \\ (z^3-c_0) \\ (z-z_0)(z^3-c_0) \\ (z^3-c_0)^2 \end{bmatrix} \mathrm{d}z \tag{11}$$

3. The solution of wave equations

It is assumed that the displacement shape function have the form (Sun and Luo 2011)

$$\begin{aligned} \left[u_0, v_0, w_0, \varphi_x, \varphi_y\right] &= \left[u^*, v^*, w^*, \varphi_x^*, \varphi_y^*\right] \\ &\times \exp[\mathrm{i}(\kappa_1 x + \kappa_2 y - \omega t)] \end{aligned} \tag{12}$$

Here, u^*, v^*, w^*, φ^*_x and φ^*_y are the wave amplitudes, κ_1 and κ_2 are the wave numbers along the $x$and y directions, substitution of Eq. (12) into Eqs. (6)-(10) leads to a matrix form, as

$$\left(\begin{bmatrix} A_{11}\kappa_1^2 + A_{66}\kappa_2^2 & (A_{12}+A_{66})\kappa_1\kappa_2 & 0 & 0 & 0 \\ (A_{12}+A_{66})\kappa_1\kappa_2 & A_{22}\kappa_2^2 + A_{66}\kappa_1^2 & 0 & 0 & 0 \\ 0 & 0 & k_{33} & k_{34} & k_{35} \\ 0 & 0 & k_{43} & k_{44} & k_{45} \\ 0 & 0 & k_{53} & k_{54} & k_{55} \end{bmatrix} \times \left[u^*, v^*, w^*, \varphi_x^*, \varphi_y^*\right]^{\mathrm{T}} \right.$$
$$\left. -\omega^2 \begin{bmatrix} I_0 & 0 & -\left(\frac{4}{3h^2}\mathrm{i}I_3\kappa_1\right) & J_1 & 0 \\ 0 & I_0 & -\left(\frac{4}{3h^2}\mathrm{i}I_3\kappa_2\right) & 0 & J_1 \\ \frac{4}{3h^2}\mathrm{i}I_3\kappa_1 & \frac{4}{3h^2}\mathrm{i}I_3\kappa_2 & I_0 + \frac{16}{9h^4}I_6\kappa_1^2 + \frac{16}{9h^4}I_6\kappa_2^2 & \frac{4}{3h^2}\mathrm{i}J_4\kappa_1 & \frac{4}{3h^2}\mathrm{i}J_4\kappa_2 \\ J_1 & 0 & -\frac{4}{3h^2}\mathrm{i}J_4\kappa_1 & K_2 & 0 \\ 0 & J_1 & -\frac{4}{3h^2}\mathrm{i}J_4\kappa_2 & 0 & K_2 \end{bmatrix} \right) = \boldsymbol{0} \tag{13}$$

in which

$$\begin{aligned} k_{33} &= A_{44}\kappa_1^2 - \frac{8}{h^2}D_{44}\kappa_1^2 + \frac{16}{h^4}F_{44}\kappa_1^2 + \frac{16}{9h^4}H_{11}\kappa_1^4 \\ &+ A_{55}\kappa_2^2 - \frac{8}{h^2}D_{55}\kappa_2^2 + \frac{16}{h^4}F_{55}\kappa_2^2 + \frac{32}{9h^4}H_{12}\kappa_1^2\kappa_2^2 \\ &+ \frac{64}{9h^4}H_{66}\kappa_1^2\kappa_2^2 + \frac{16}{9h^4}H_{22}\kappa_2^4 \\ k_{34} &= \frac{8}{h^2}\mathrm{i}D_{44}\kappa_1 - \mathrm{i}A_{44}\kappa_1 - \frac{16}{h^4}\mathrm{i}F_{44}\kappa_1 + \frac{4}{3h^2}\mathrm{i}F_{11}\kappa_1^3 \\ &- \frac{16}{9h^4}\mathrm{i}H_{11}\kappa_1^3 + \frac{4}{3h^2}\mathrm{i}F_{12}\kappa_1\kappa_2^2 + \frac{8}{3h^2}\mathrm{i}F_{66}\kappa_1\kappa_2^2 \\ &- \frac{16}{9h^4}\mathrm{i}H_{12}\kappa_1\kappa_2^2 - \frac{32}{9h^4}H_{66}\kappa_1\kappa_2^2 \\ k_{35} &= \frac{8}{h^2}\mathrm{i}D_{55}\kappa_2 - \mathrm{i}A_{55}\kappa_2 - \frac{16}{h^4}\mathrm{i}F_{55}\kappa_2 \\ &+ \frac{4}{3h^2}\mathrm{i}F_{12}\kappa_1^2\kappa_2 + \frac{8}{3h^2}\mathrm{i}F_{66}\kappa_1^2\kappa_2 - \frac{16}{9h^4}\mathrm{i}H_{12}\kappa_1^2\kappa_2 \\ &- \frac{32}{9h^4}\mathrm{i}H_{66}\kappa_1^2\kappa_2 + \frac{4}{3h^2}\mathrm{i}F_{22}\kappa_2^3 - \frac{16}{9h^4}\mathrm{i}H_{22}\kappa_2^3 \end{aligned} \tag{14}$$

$$\begin{aligned} k_{43} &= \mathrm{i}A_{44}\kappa_1 - \frac{8}{h^2}\mathrm{i}D_{44}\kappa_1 + \frac{16}{h^4}\mathrm{i}F_{44}\kappa_1 - \frac{4}{3h^2}\mathrm{i}F_{11}\kappa_1^3 \\ &- \frac{4}{3h^2}\mathrm{i}F_{12}\kappa_1\kappa_2^2 - \frac{8}{3h^2}\mathrm{i}F_{66}\kappa_1\kappa_2^2 + \frac{16}{9h^4}\mathrm{i}H_{12}\kappa_1\kappa_2^2 \\ &+ \frac{32}{9h^4}\mathrm{i}H_{66}\kappa_1\kappa_2^2 + \frac{16}{9h^4}\mathrm{i}H_{11}\kappa_1^3 \\ k_{44} &= A_{44} - \frac{8}{h^2}D_{44} + \frac{16}{h^4}F_{44} + \frac{16}{9h^4}H_{66}\kappa_2^2 \\ &- \frac{8}{3h^2}F_{11}\kappa_1^2 + \frac{16}{9h^4}H_{11}\kappa_1^2 + D_{66}\kappa_2^2 \\ &- \frac{8}{3h^2}F_{66}\kappa_2^2 + D_{11}\kappa_1^2 \\ k_{45} &= D_{12}\kappa_1\kappa_2 - \frac{8}{3h^2}F_{12}\kappa_1\kappa_2 + D_{66}\kappa_1\kappa_2 \\ &- \frac{8}{3h^2}F_{66}\kappa_1\kappa_2 + \frac{16}{9h^4}H_{12}\kappa_1\kappa_2 + \frac{16}{9h^4}H_{66}\kappa_1\kappa_2 \\ k_{53} &= \mathrm{i}A_{55}\kappa_2 - \frac{8}{h^2}\mathrm{i}D_{55}\kappa_2 + \frac{16}{h^4}\mathrm{i}F_{55}\kappa_2 \\ &- \frac{4}{3h^2}\mathrm{i}c_1F_{12}\kappa_1^2\kappa_2 - \frac{8}{3h^2}\mathrm{i}F_{66}\kappa_1^2\kappa_2 + \frac{16}{9h^4}\mathrm{i}H_{12}\kappa_1^2\kappa_2 \\ &+ \frac{32}{9h^4}\mathrm{i}H_{66}\kappa_1^2\kappa_2 - \frac{4}{3h^2}\mathrm{i}F_{22}\kappa_2^3 + \frac{16}{9h^4}\mathrm{i}H_{22}\kappa_2^3 \\ k_{54} &= D_{12}\kappa_1\kappa_2 - \frac{8}{h^2}F_{12}\kappa_1\kappa_2 + D_{66}\kappa_1\kappa_2 \\ &- \frac{8}{3h^2}F_{66}\kappa_1\kappa_2 + \frac{16}{9h^4}H_{12}\kappa_1\kappa_2 + \frac{16}{9h^4}H_{66}\kappa_1\kappa_2 \\ k_{55} &= A_{55} - \frac{8}{h^2}D_{55} + \frac{16}{h^4}F_{55} + D_{22}\kappa_2^2 - \frac{8}{3h^2}F_{11}\kappa_2^2 \\ &+ \frac{16}{9h^4}H_{22}\kappa_2^2 + D_{66}\kappa_1^2 - \frac{8}{3h^2}F_{66}\kappa_1^2 + \frac{16}{9h^4}H_{66}\kappa_1^2 \end{aligned}$$

If we want Eq. (13) to have a nonzero solution, then the value of the coefficient determinants of Eq. (13) must be 0, from which, we can find five roots of circular frequency, two of which are for longitudinal wave, the other two for shear wave and one for bending wave. The expressions of phase velocity and group velocity can be obtained by the following expressions,

$$C_i = \frac{\omega_i(\kappa)}{\kappa},\ C_{g_i} = \frac{\mathrm{d}\omega_i(\kappa)}{\mathrm{d}\kappa}\ (i = 1,2,3,4,5) \tag{15}$$

4. Examples

Since there are five different forms of elastic waves in this FGM plate, we need to analyze five different cases. Before carrying out the numerical analysis, we first verify the correctness of this study. When the pore volume fraction is 0, the curves of the degenerated circular frequency, phase velocity and group velocity are compared with the results of the existing literature. See Fig. 2 for details. Through comparison, the correctness of this paper is verified. In addition, we also find in Fig. 2 that the phase velocity and group velocity decrease with the increase of functionally graded index.

In addition, in Fig. 3 to Fig. 5, we study the influence of pore volume fraction on phase velocity, group velocity and circular frequency. During the calculation, we take N = 0.5 and N = 2. We find that when N = 0.5, the increase of pore

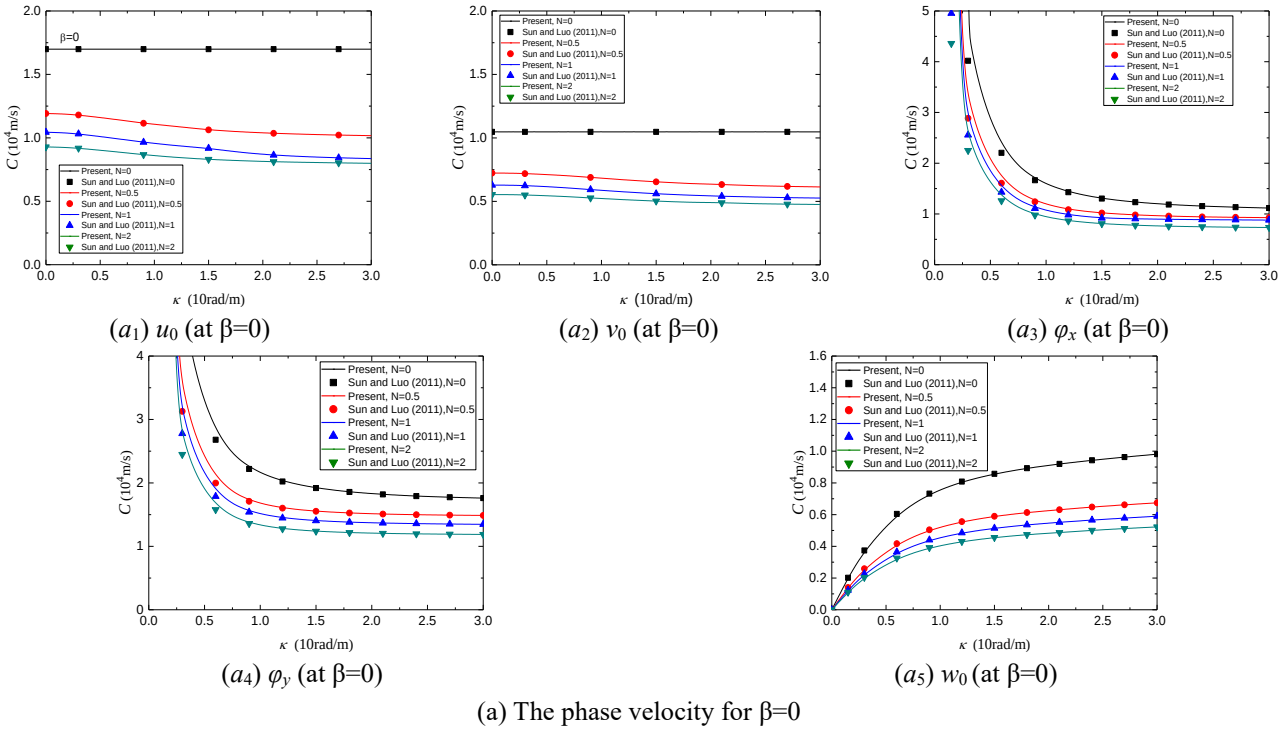

(a_1) u_0 (at β=0) (a_2) v_0 (at β=0) (a_3) φ_x (at β=0)

(a_4) φ_y (at β=0) (a_5) w_0 (at β=0)

(a) The phase velocity for β=0

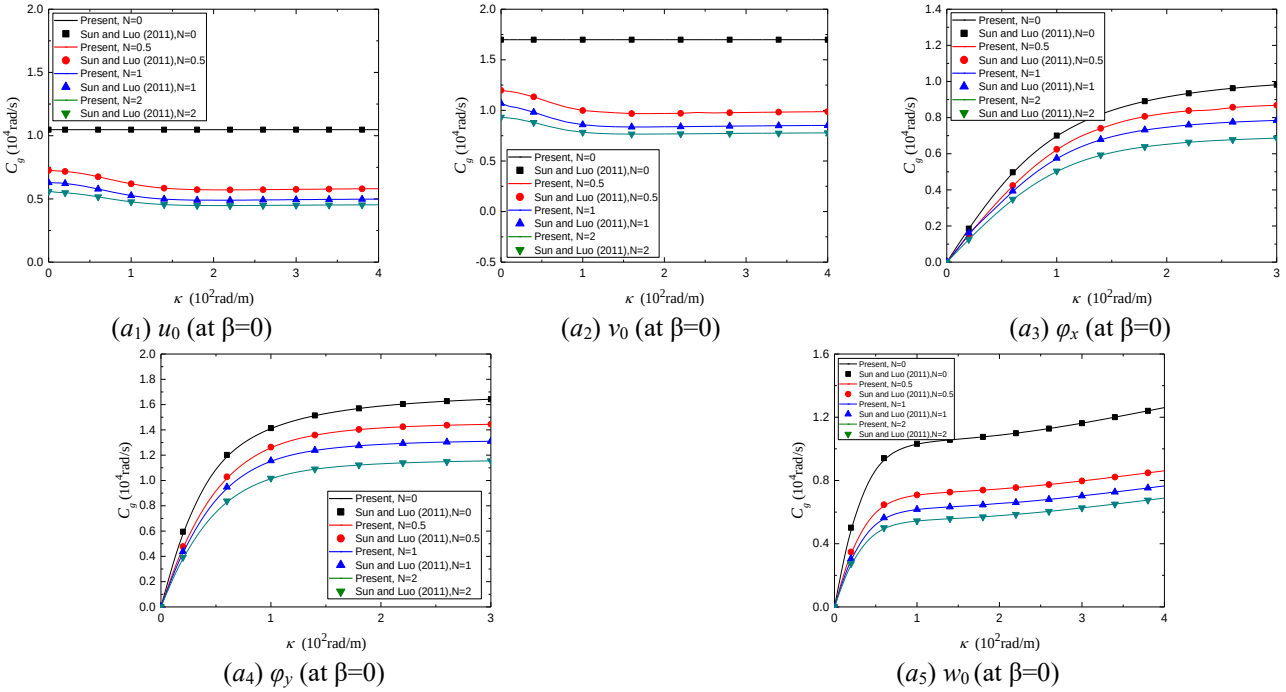

(a_1) u_0 (at β=0) (a_2) v_0 (at β=0) (a_3) φ_x (at β=0)

(a_4) φ_y (at β=0) (a_5) w_0 (at β=0)

(b) The group velocity for β=0

Fig. 2 Comparison with the existing results (Sun and Luo 2011), (a) The phase velocity for β=0 and (b) The group velocity for β=0

volume fraction will lead to the increase of phase velocity, group velocity and circular frequency. However, when N = 2, we find that the effect of pore volume fraction on phase velocity is different, In other words, the phase velocity, group velocity, and circular frequency decrease with the increase of pore volume fraction.

In addition, we also find that the shapes of shear wave and are almost the same, while the shapes of P-wave and are almost the same.

5. Conclusions

The wave propagations of the porous FG plates based on Reddy's higher order shear deformation and physical neutral surface concept have been studied in this paper. The wave propagation analyses are solved using trial function. The correctness of this paper has been verified by comparing with the existing results. The numerical analyses shows that:

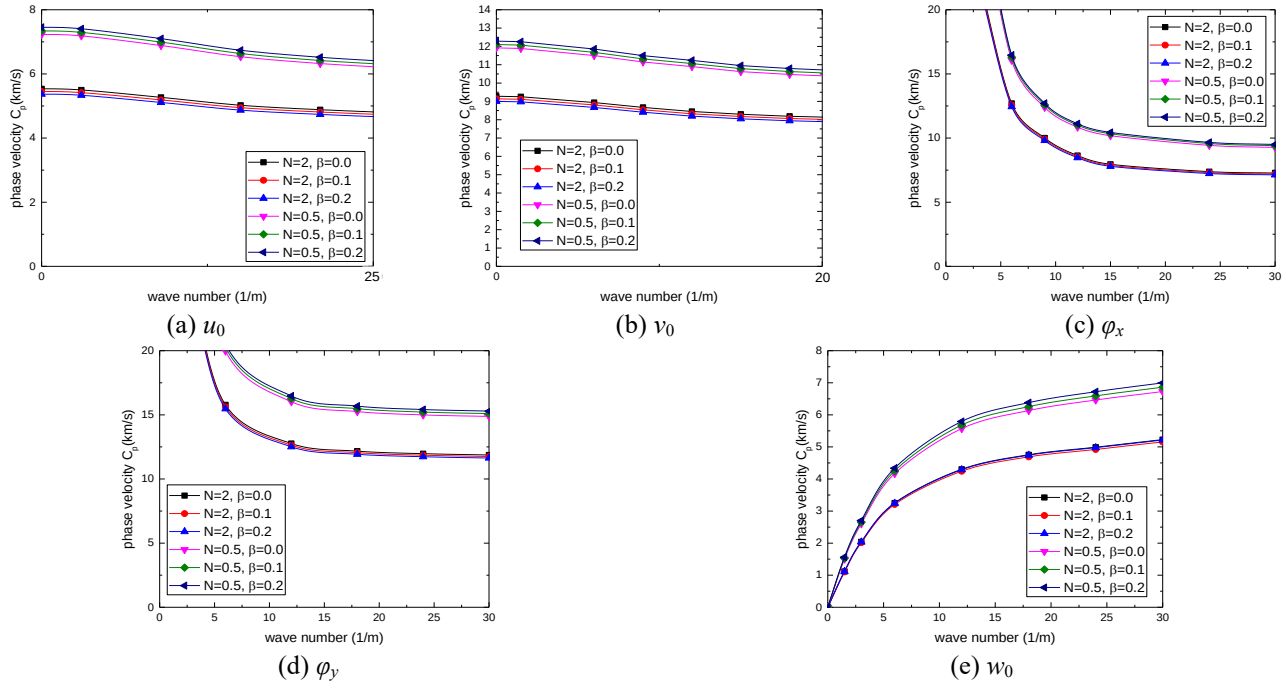

(a) u_0 (b) v_0 (c) φ_x

(d) φ_y (e) w_0

Fig.3 Effect of the porosity on the phase velocity

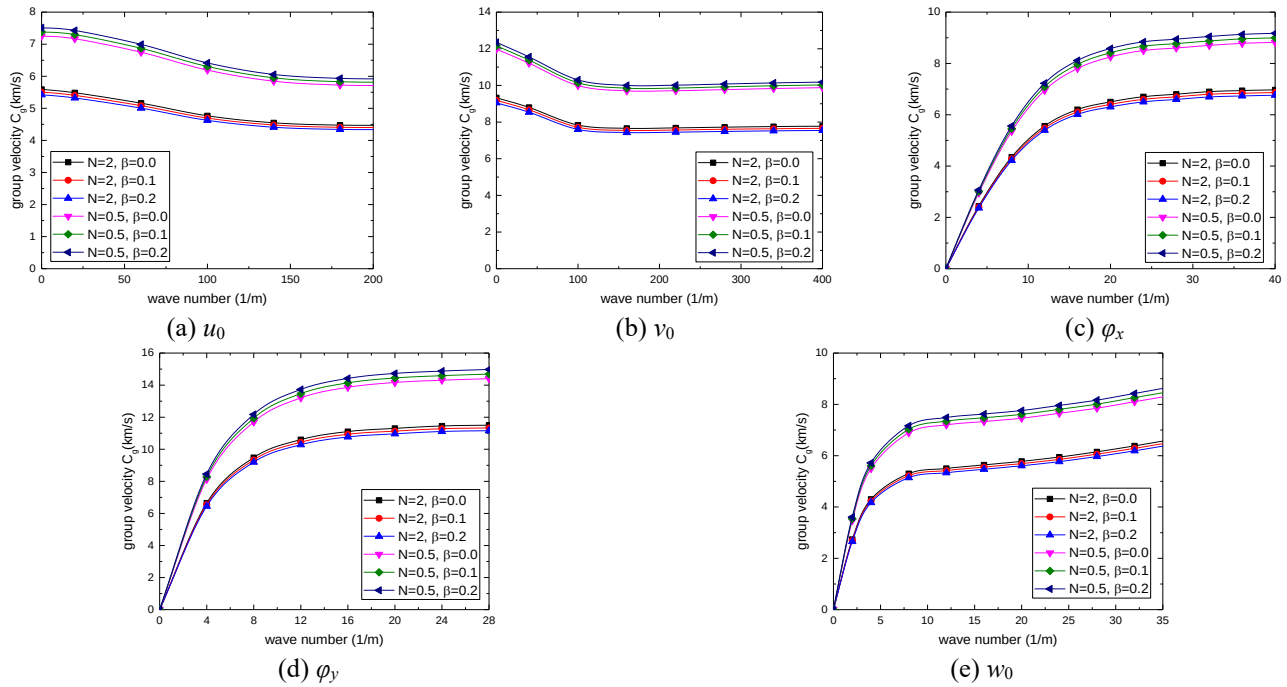

(a) u_0 (b) v_0 (c) φ_x

(d) φ_y (e) w_0

Fig. 4 Effect of the porosity on the group velocity

- When N= 0.5, the increase of pore volume fraction will lead to the increase of phase velocity, group velocity and circular frequency. However, when N = 2, we find that pore volume fraction has inhibitory effect on phase velocity, group velocity and circular frequency. That is to say, when pore volume fraction increases, phase velocity, group velocity and circular frequency will decrease. This shows that porosity is a very complex factor in the analysis of wave propagation.

- In the process of increasing the functional gradient index, the circular frequency, phase velocity and group velocity will decrease.

- The shapes of shear wave and are almost the same, while the shapes of P-wave and are almost the same.

Authorship contribution statement

Hang Xiao: Theoretical modeling and computation;

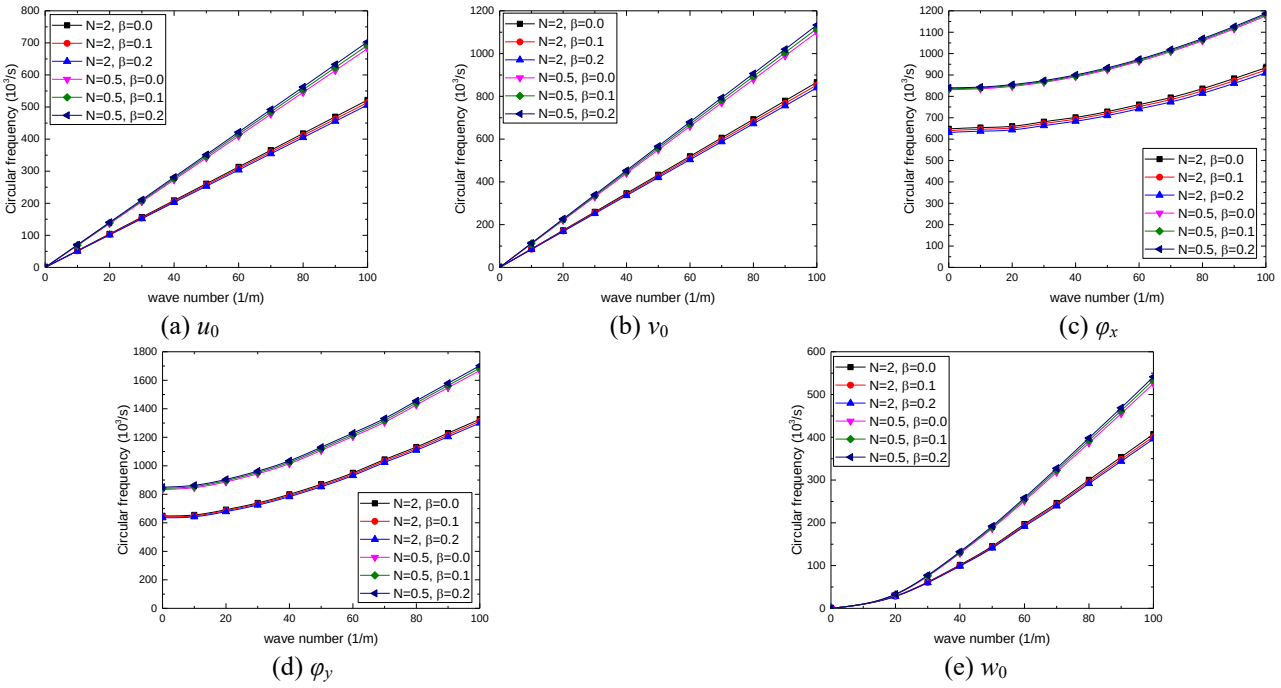

Fig. 5 Effect of the porosity on the circular frequency

Textwriting of the whole article, Editing and Revising & Writeprogram;

Kunming Yan: Writing-review, Discussion and analysis.

Guilin She: Providing guidance, Investigation, Discussion & Guidance

References

Ahmadi, H. and Foroutan, K. (2019), "Combination resonance analysis of FG porous cylindrical shell under two-term excitation", *Steel Compos. Struct.*, **32**(2), 253-264. http://doi.org/10.12989/scs.2019.32.2.253.

Ahmed, A., Fenjan, R.M. and Faleh, N.M. (2019), "Analyzing post-buckling behavior of continuously graded FG nanobeams with geometrical imperfections", *Geomech. Eng.*, **17**(2), 175-180. http://doi.org/10.12989/gae.2019.17.2.175.

Alnujaie, A., Akbas, S.D., Eltaher, M.A. and Assie, A. (2021), "Forced vibration of a functionally graded porous beam resting on viscoelastic foundation", *Geomech. Eng.*, **24**(1), 91-103. http://doi.org/10.12989/gae.2021.24.1.091

Arefi, M. and Meskini, M. (2019), "Application of hyperbolic shear deformation theory to free vibration analysis of functionally graded porous plate with piezoelectric face-sheets", *Struct. Eng. Mech.*, **71**(5), 459-467. http://doi.org/10.12989/sem.2019.71.5.459.

Arefi, M., Kiani, M. and Rabczuk, T. (2019), "Application of nonlocal strain gradient theory to size dependent bending analysis of a sandwich porous nanoplate integrated with piezomagnetic face-sheets", *Compos. Part B Eng.*, **168**, 320-333. http://doi.org/10.1016/j.compositesb.2019.02.057.

Arefi, M., Firouzeh, S., Bidgoli, E.M.R., and Civalek, O. (2020), "Analysis of porous micro-plates reinforced with FG-GNPs based on Reddy plate theory", *Compos. Struct.*, **247**(1), 112391. https://doi.org/10.1016/j.compstruct.2020.112391.

Arefi, M. and Zenkour, A.M. (2017), "Wave propagation analysis of a functionally graded magneto-electro-elastic nanobeam rest on Visco-Pasternak foundation", *Mech. Res. Commun.*, **79**, 51-62. https://doi.org/10.1016/j.mechrescom.2017.01.004.

Arefi, M. (2016), "Analysis of wave in a functionally graded magneto-electro-elastic nano-rod using nonlocal elasticity model subjected to electric and magnetic potentials", *Acta Mech.*, **227**(9), 2529-2542. https://doi.org/10.1007/s00707-016-1584-7.

Arshid, E., Khorshidvand, A.R. and Khorsandijou, S.M. (2019), "The effect of porosity on free vibration of SPFG circular plates resting on visco-Pasternak elastic foundation based on CPT, FSDT and TSDT", *Struct. Eng. Mech.*, **70**(1), 97-112. http://doi.org/10.12989/sem.2019.70.1.097.

Avcar, M. (2019), "Free vibration of imperfect sigmoid and power law functionally graded beams", Steel Compos. Struct., 30(6), 603-615. http://dx.doi.org/10.12989/scs.2019.30.6.603

Bamdad, M., Mohammadimehr, M., and Alambeigi, K. (2020), "Bending and buckling analysis of sandwich Reddy beam considering shape memory alloy wires and porosity resting on Vlasov's foundation", *Steel Compos. Struct.*, **36**(6), 671-687. http://doi.org/10.12989/scs.2020.36.6.671

Barretta, R. and de Sciarra, F.M. (2019), "Variational nonlocal gradient elasticity for nano-beams", *Int. J. Eng. Sci.*, **143**, 73-91. https://doi.org/10.1016/j.ijengsci.2019.06.016.

Batou, B., Nebab, M., Bennai, R., Atmane, H.T., Tounsi, A. and Bouremana, M. (2019), "Wave dispersion properties in imperfect sigmoid plates using various HSDTs", *Steel Compos. Struct.*, **33**(5), 699-716. http://doi.org/10.12989/scs.2019.33.5.699.

Benahmed, A., Fahsi, B., Benzair, A., Zidour, M., Bourada, F. and Tounsi, A. (2019), "Critical buckling of functionally graded nanoscale beam with porosities using nonlocal higher-order shear deformation", *Struct. Eng. Mech.*, **69**(4), 457-466. http://doi.org/10.12989/sem.2019.69.4.457.

Bennai, R., Fourn, H., Atmane, H.A., Tounsi, A. and Bessaim, A. (2019), "Dynamic and wave propagation investigation of FGM plates with porosities using a four variable plate theory", *Wind Struct.*, **28**(1), 49-62. https://doi.org/10.12989/was.2019.28.1.049.

Civalek, O., Uzun, B., Yaylı, M.O. and Akgöz, B. (2020), "Sizedependent transverse and longitudinal vibrations of

embedded carbon and silica carbide nanotubes by nonlocal finite element method", *Eur. Phys. J. Plus*, **135**, 381. https://doi.org/10.1140/epjp/s13360-020-00385-w.

Ebrahim, F., Jafaril, A., and Mahesh, V. (2019), "Assessment of porosity influence on dynamic characteristics of smart heterogeneous magneto-electro-elastic plates", *Struct. Eng. Mech.*, **72**(1), 113-129. http://doi.org/10.12989/sem.2019.72.1.113

Ebrahimi, F. and Seyfi, A. (2020), "Studying propagation of wave of metal foam rectangular plates with graded porosities resting on Kerr substrate in thermal environment via analytical method", Wave Random Complex. https://doi.org/10.1080/17455030.2020.1802531

Faghidian, S.A. (2021), "Contribution of nonlocal integral elasticity to modified strain gradient theory", *Eur. Phys. J. Plus*, **136**(5), 559. https://doi.org/10.1140/epjp/s13360-021-01520-x

Faghidian, S.A. (2020), "Higher-order nonlocal gradient elasticity: A consistent variational theory", *Int. J. Eng. Sci.*, **154**, 103337. https://doi.org/10.1016/j.ijengsci.2020.103337.

Fenjan, R.M., Faleh, N.M. and Ridha, A.A. (2020), "Strain gradient based static stability analysis of composite crystalline shell structures having porosities", *Steel Compos. Struct.*, **36**(6), 631-642. http://doi.org/10.12989/scs.2020.36.6.631.

Gao, W., Qin, Z. and Chu, F. (2020), "Wave propagation in functionally graded porous plates reinforced with graphene platelets", *Aerosp. Sci. Technol.*, **102**, 105860. https://doi.org/10.1016/j.ast.2020.105860.

Ghandourh, E.E. and Abdraboh, A.M. (2020), "Dynamic analysis of functionally graded nonlocal nanobeam with different porosity models", *Steel Compos. Struct.*, **36**(3), 293-305. http://doi.org/10.12989/scs.2020.36.3.293.

Ghayesh, M.H. and Farokhi, H. (2020), "Extremely large dynamics of axially excited cantilevers", *Thin Walled Struct.*, **154**, 106275. http://doi.org/10.1016/j.tws.2019.106275.

Farokhi, H. and Ghayesh, M.H. (2020), "Motion limiting nonlinear dynamics of initially curved beams", *Thin Walled Struct.*, **158**, 106346. http://doi.org/10.1016/j.tws.2019.106346.

Hadj, B., Rabia, B., Daouadji, T.H. (2019), "Influence of the distribution shape of porosity on the bending FGM new plate model resting on elastic foundations", *Struct. Eng. Mech.*, **72**(1), 61-70. http://doi.org/10.12989/sem.2019.72.1.061

Hadji, L., Zouatnia, N. and Bernard, F. (2019), "An analytical solution for bending and free vibration responses of functionally graded beams with porosities: Effect of the micromechanical models", *Struct. Eng. Mech.*, **69**(2), 231-241. http://doi.org/10.12989/sem.2019.69.2.231.

Hamed, M.A., Sadoun, A.M. and Eltaher, M.A. (2019), "Effects of porosity models on static behavior of size dependent functionally graded beam", *Struct. Eng. Mech.*, **71**(1), 89-98. http://doi.org/10.12989/sem.2019.71.1.089

Jalaei, M.H. and Civalek, Ö. (2019), "On dynamic instability of magnetically embedded viscoelastic porous FG nanobeam", *Int. J. Eng. Sci.*, **143**, 14-32. https://doi.org/10.1016/j.ijengsci.2019.06.013.

Jia, A., Liu, H., Ren, L., Yun, Y. and Tahouneh, V. (2020), "Influence of porosity distribution on vibration analysis of GPLs-reinforcement sectorial plate", *Steel Compos. Struct.*, **35**(1), 111-127. http://doi.org/10.12989/scs.2020.35.1.111.

Khazaei, P. and Mohammadimehr, M. (2020), "Size dependent effect on deflection and buckling analyses of porous nanocomposite plate based on nonlocal strain gradient theory", *Struct. Eng. Mech.*, **76**(1), 27-56. http://doi.org/10.12989/sem.2020.76.1.027.

Liang, C. and Wang, Y.Q. (2020), "A quasi-3D trigonometric shear deformation theory for wave propagation analysis of FGM sandwich plates with porosities resting on viscoelastic foundation", *Compos. Struct.*, **247**, 112478. https://doi.org/10.1016/j.compstruct.2020.112478.

Lu, L., She, G.L. and Guo, X. (2021a), "Size-dependent postbuckling analysis of graphene reinforced composite microtubes with geometrical imperfection", *Int. J. Mech. Sci.*, **199**, 106428. https://doi.org/10.1016/j.ijmecsci.2021.106428.

Lu, L., Wang, S., Li, M. and Guo, X. (2021b), "Free vibration and dynamic stability of functionally graded composite microtubes reinforced with graphene platelets", *Compos. Struct.*, **272**(15), 114231. https://doi.org/10.1016/j.compstruct.2021.114231.

Lu, L., Zhu, L., Guo, X., Zhao, J. and Liu, G. (2019), "A nonlocal strain gradient shell model incorporating surface effects for vibration analysis of functionally graded cylindrical nanoshells", *Appl. Math. Mech.*, **40**(12), 1695-1722. https://doi.org/10.1007/s10483-019-2549-7.

Malikan, M., Krasheninnikov, M., Eremeyev, V.A. (2020b), "Torsional stability capacity of a nano-composite shell based on a nonlocal strain gradient shell model under a three-dimensional magnetic field", Int. J. Eng. Sci., 148, 103210. http://dx.doi.org/10.1016/j.ijengsci.2019.103210

Malikan, M., Uglov, N.S. and Eremeyev, V.A. (2020a), "Oninstabilities and post-buckling of piezomagnetic andflexomagnetic nanostructures", *Int. J. Eng. Sci.*, **157**, 103395. http://doi.org/10.1016/j.ijengsci.2020.103395.

Mekerbi, M., Benyoucef, S., Mahmoudi, A., Bourada, F., and Tounsi, A. (2019), "Investigation on thermal buckling of porous FG plate resting on elastic foundation via quasi 3D solution", *Struct. Eng. Mech.*, **72**(4), 513-524. http://doi.org/10.12989/sem.2019.72.4.513.

Mirjavadi, S.S., Forsat, M., Yahya, Y.Z., Barati, M.R., Jayasimha, A.N. and Hamouda, A.M.S. (2020), "Porosity effects on post-buckling behavior of geometrically imperfect metal foam doubly-curved shells with stiffeners", *Struct. Eng. Mech.*, **75**(6), 701-711. http://doi.org/10.12989/sem.2020.75.6.701.

Nebab, M., Atmane, H.A., Bennai, R., Tounis., A. and Bedia, E.A.A. (2019), "Vibration response and wave propagation in FG plates resting on elastic foundations using HSDT", *Struct. Eng. Mech.*, **69**(5), 511-525. https://doi.org/10.12989/sem.2019.69.5.511.

Rabia, B., Daouadji, T.H. and Abderezak, R. (2019), "Effect of porosity in interfacial stress analysis of perfect FGM beams reinforced with a porous functionally graded materials plate", *Struct. Eng. Mech.*, **72**(3), 293-304. http://doi.org/10.12989/sem.2019.72.3.293.

Rahmani, M., Mohammadi, Y. and Kakavand, F. (2019), "Vibration analysis of sandwich truncated conical shells with porous FG face sheets in various thermal surroundings", *Steel Compos. Struct.*, **32**(2), 239-252. http://doi.org/10.12989/scs.2019.32.2.239.

Sadoughifar, A., Farhatnia, F., Izadinia, M. and Tal, S.B. (2019), "Nonlinear bending analysis of porous FG thick annular/circular nanoplate based on modified couple stress and two-variable shear deformation theory using GDQM", *Steel Compos. Struct.*, **33**(2), 307-318. http://doi.org/10.12989/scs.2019.33.2.307.

Sadoughifar, A., Farhatnia, F., Izadinia, M. and Talaeetaba, S.B. (2020), "Size-dependent buckling behaviour of FG annular/circular thick nanoplates with porosities resting on Kerr foundation based on new hyperbolic shear deformation theory", *Struct. Eng. Mech.*, **73**(3), 225-238. http://doi.org/10.12989/sem.2020.73.3.225.

She, G.L., Liu, H.B. and Karami, B. (2021), "Resonance analysis of composite curved microbeams reinforced with graphene nanoplatelets", *Thin Wall. Struct.*, **160**, 107407. https://doi.org/10.1016/j.tws.2020.107407

Sun, D. and Luo, S.N. (2011), "Wave propagation of functionally graded material plates in thermal environments", *Ultrasonics*, **51**(8), 940-952. http://doi.org/10.1016/j.ultras.2011.05.009.

Xu, K., Yuan, Y. and Li, M. (2019), "Buckling behavior of

functionally graded porous plates integrated with laminated composite faces sheets", *Steel Compos*. *Struct*., **32**(5), 633-642. http://doi.org/10.12989/scs.2019.32.5.633.

Yahia, S.A., Atmane, H.A., Houari, M.S.A, and Tounis., A. (2019), "Wave propagation in functionally graded plates with porosities using various higher-order shear deformation plate theories", *Struct*. *Eng*. *Sci*., **53**(6), 1143-1165. https://doi.org/10.12989/sem.2015.53.6.1143.

Zhang, D.G. (2013), "Modeling and analysis of FGM rectangular plates based on physical neutral surface and high order shear deformation theory", *Int*. *J*. *Mech*. *Sci*., **68**, 92-104. http://doi.org/10.1016/j.ijmecsci.2013.01.002.

Zhang, D.G. (2014), "Nonlinear bending analysis of FGM rectangular plates with various supported boundaries resting on two-parameter elastic foundations", *Arch*. *Appl*. *Mec*h., **84**(1), 1-20. http://doi.org/10.1007/s00419-013-0775-0.

Zhang, Y.Y., Wang, X.Y., Zhang, X., Shen, H.M., and She, G.L. (2021), "On snap-buckling of FG-CNTR curved nanobeams considering surface effects", *Steel Compos*. *Struct.*, **38**(3), 293-304. https://doi.org/10.12989/scs.2021.38.3.293.

JS